

Performance Evaluation of Triple-band Microstrip Antenna using Hybrid-SRRs on Truncated Ground Plane

Varun Setia,^{#,*} Kamalesh Kumar Sharma,[#] and Shibhan Kishan Koul[§]

[#]Department of Electronics and Communication Engineering, Malaviya National Institute of Technology, Jaipur - 302017, India

[§]Center for Applied Research in Electronics, IIT Delhi - 110016, India

*E-mail: 2015rec9538@mnit.ac.in

ABSTRACT

A single-band monopole antenna, transformed into a triple-band antenna for S-band and C-band applications is reported in this paper. This transformation is done with the help of two different hybrid SRR unit cells, which are embedded on the truncated ground plane of the antenna. These hybrid SRR unit cells are created by combining square split ring and circular split ring into two different configurations. Simulated results are in coherence with the measured results and analysis is provided to evaluate the efficacy of the design. This analysis can be used to estimate the usefulness of metamaterial unit cells in generating multiple frequency bands. The operating frequency bands measured are 2.72-2.83GHz, 3.54-4.35 GHz, and 4.72-5 GHz respectively. These bands are being used in the mid-band frequency range of 5G communication in many countries. The developed antenna is miniaturized to the size of $0.19\lambda_0 \times 0.25\lambda_0$ (λ_0 is the free space wavelength at 2.72 GHz). Two objectives i.e., miniaturization and multi-banding are fulfilled in a single design. The introduction of different hybrid SRR unit cells at defective ground plane causes multi-banding and resonance of a unit cell at a lower frequency leads to an increase in the effective electrical length of the antenna without increasing its physical size. The metamaterial characteristic of the unit cells is also verified in the article.

Keywords: Hybrid-SRR; Metamaterial unit cell; Triple-band antenna; Truncated ground

1. INTRODUCTION

Miniaturized multi-band microstrip antenna has always been in demand for integrating different wireless applications with a single antenna. These applications could be WLAN, RFID, WiMax, wireless energy harvesting, wireless sensor networks, 5G MIMO, etc. Also, a single antenna can be used to accommodate various wireless standards together. So, it is very much desirable that many antenna for different applications be substituted by a single multi-band antenna in order to optimally utilize the space. There are several techniques available to miniaturize the size of antenna such as using fractal shapes, meandered lines, defected grounds, metamaterials, etc., for which comprehensive review is available in reference 1. Many of these techniques are explored in the literature to achieve multi-band operation. A triple-band monopole antenna using a slot of fractal Koch is reported in reference 2. A monopole antenna having the crinkle fractal design is discussed in reference 3. The advantage of using a monopole antenna is in achieving larger impedance bandwidth. A compact-sized transparent antenna which is again a triple band monopole antenna is proposed in reference 4. A multi-layer multi-ring antenna fed by an L-probe, generating a triple band is simulated in reference 5. The ground plane of the monopole antenna is

modified in reference 6 to achieve an additional frequency band. A triple-band antenna consisting of spiral-shaped radiators along with a slot radiator is presented in reference 7. A triple-band antenna using an open hexagonal-shaped radiator with the defected ground is reported in reference 8. To optimize the space, an aperture shared triple-band antenna is presented in reference 9. Since a multi-band antenna is highly demanded in 5G MIMO applications, a triple-band antenna with its four modules is demonstrated in reference 10.

Another approach for obtaining multiband characteristics from a single antenna with compact size is based on metamaterial structures. These structures provide easy modeling and better frequency control during optimization which is discussed in the later sections of this paper. As the metamaterial structures are sub-wavelength structures, a significant amount of reduction in antenna size can be achieved¹¹⁻¹³.

Metamaterials are not found naturally but are created generally as 2-D or 3-D periodic structures. These structures show a negative refractive index for a definite frequency range. The concept of the negative refractive index for a substance was hypothesized by Veselago in 1967¹¹. Later, Pendry, *et al.* demonstrated this phenomenon for thin metallic wires and other structures.¹²⁻¹³ And since, negative refraction is not usual, these structures were termed "Metamaterials". An ample amount of information about the history and development of metamaterials can be found in reference 14-19 for further

exploration. A single unit of these structures is called a unit cell. The complete effect of the whole metamaterial structure can be estimated just by studying its unit cell's behavior with proper boundary conditions^{15,17}.

Nowadays, it is very popular to use a separate unit cell instead of using a full periodic structure. Most of the time, these unit cells are Split-Ring Resonators (SRRs) of various shapes. SRRs have been proved to be a good choice for multi-banding, gain enhancement, antenna miniaturization, absorbers, and notch antenna. The SRRs show negative permeability which ultimately leads to negative refraction. If only a few unit cells are used with an antenna structure instead of using a full periodic structure, these designs can be termed metamaterial-inspired designs because the metamaterial property is verified for a single unit cell. Many metamaterial-inspired antenna for different microwave applications have been reported in the literature. A state-of-the-art literature review of antenna utilizing the metamaterial concept for multi-banding and miniaturization is presented here.

A frequency reconfigurable antenna using two different sized double square SRR unit cells is proposed by Cheribi *et al.*²⁰ In another approach, a multi-layer metamaterial is added in close proximity to a monopole antenna in order to create additional resonance²¹. A loop-slot triple-band antenna using only a single unit of SRR is proposed in reference 22. Patel and Kosta²³ presented a complementary SRR based antenna for multi-frequency operation. A metamaterial-inspired dual-band antenna for mobile applications is discussed in reference 24. A CPW-fed monopole antenna to realize triple-band employing SRR coupling is designed in reference 25. A family of metamaterial-inspired inverted L-shaped dipole antenna is fabricated and investigated reference 26. A dual-band monopole antenna with six SRR unit cells loaded on its truncated ground plane is reported in reference 27. A dual-band MIMO antenna comprising of four-element SRR unit cells for 4G and 5G applications is presented in reference 28. A miniaturized multi-band antenna using a metamaterial-inspired unit cell is reported in reference 29. A complementary SRR loaded antenna for WLAN and IoT applications is presented in reference 30. A horizontally polarized WiFi antenna having a 3-D structure is proposed in reference 31, while a triple-band antenna using a square CSRR and two novel SCSRR is presented in reference 32.

Earlier the authors have proposed a triple band monopole antenna using two identical double square SRR unit cells on the truncated ground plane³³. In the presented work, metamaterial unit cells are a combination of the square and the circular-shaped split-ring resonators referred to as hybrid-SRR, used to obtain multi-banding and miniaturization simultaneously. The implementation of hybrid-SRRs gives more freedom to control the frequency separation between different bands. The observations show that the proposed unit cell has negative magnetic permeability (μ) and negative refractive index (n) at a lower frequency as compared to conventional metamaterial structures based on square and circular split rings, which is further verified in the latter section. It's always been a challenging task to achieve multi-banding, broad-banding, and miniaturization

together. The proposed structure is a successful attempt in this direction, where both of the benefits of using metamaterials i.e. miniaturization as well as multi-banding, are exploited. Also, a significant amount of bandwidth of 4 %, 20 %, and 6 % for the respective three frequency bands 2.8/4/4.8 GHz is achieved. The complexity level has been kept low in the proposed design. Hence, a stable antenna is presented.

Utilizing these hybrid-SRRs, a single band monopole antenna is converted into a triple-band antenna. Its feasibility, potential, and performance are investigated in this paper.

The structure of the paper is as follows. Section one is the introduction which discusses the motivation behind this work. The usefulness and novelty of the present work are also discussed in this section. Section two deals with the antenna geometry, the evolution of hybrid-SRRs, and the role of metamaterial unit cells to achieve multi-banding and miniaturization. The experimental results are discussed in section three followed by the comparison with state-of-the-art literature. Finally, the conclusion and future scope of the presented work are given in section four.

2. ANTENNA DESIGN

2.1 Geometry

The presented antenna design consists of a rectangular metallic patch engraved upon the FR4 substrate (having the relative permittivity of 4.4) as shown in Figure 1(a). On the backside of the substrate which is a truncated ground plane, two different hybrid-SRR metamaterial unit cells are loaded as shown in Fig. 1 (b). The substrate thickness is chosen to be 1.524 mm. Simulation work for antenna design and optimization is accomplished by the Ansys HFSS software package. Both of

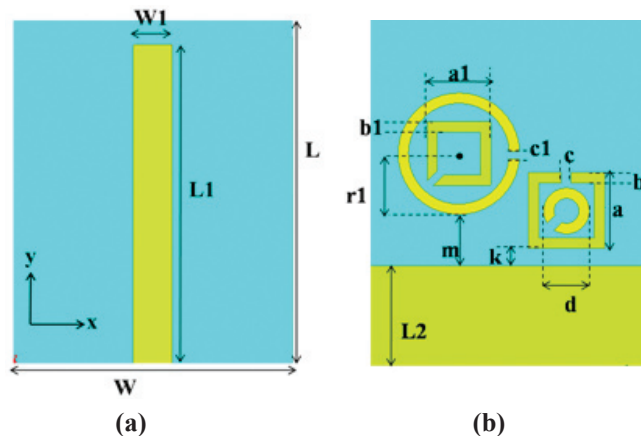


Figure 1. Schematic diagram of the proposed antenna: (a) Top view, and (b) Bottom view.

the SRR structures are designed separately and corresponding dimensions are optimized through parametric studies. The orientation of the split is kept at 45 ° for inner rings in both of the SRR structures.

All dimensions of the proposed antenna are indicated in Fig. 1 and their corresponding values (in millimeter) are given in Table 1.

Resonating frequency of the metamaterial unit cell is dependent on its overall dimension and the inter-ring spacing. While using these rings on a defective ground plane, many of the ring parameters help in impedance matching without

affecting the resonant frequency. This is discussed in detail in the next section where the analysis of hybrid-SRR is given.

Table 1. Antenna parameters

Parameter	Value	Parameter	Value
W	22	d	3.6
L	28	k	1.4
W1	3	m	6.9
L1	26	r1	4.8
L2	8	a1	5
a	6	b1	0.8
b	0.8	c1	0.6
c	0.8		

2.2 EVOLUTION OF HYBRID-SRR

The evolution steps of the proposed hybrid-SRR are shown in Fig. 2 (a)-(c). A conventional double square SRR is taken as the initial design referred to as SRR1, later the inner square ring is replaced with a circular ring referred to as SRR2. Finally, the inner ring is rotated by 45° in SRR3. The scattering parameters for all these design steps are shown in Fig. 2(d). It can be observed that for the proposed hybrid-SRR, the crossover point of reflection and transmission coefficients shifts towards a lower frequency as compared to the conventional SRR. It is

also observed that the orientation of the split has nothing much to do with the resonating frequency rather it affects the quality of resonance. Its orientation was varied to achieve proper impedance matching for the desired frequency bands.

2.3 Unit Cell Simulation and Verification of Metamaterial Property

Now, based on the above discussion, a hybrid SRR is designed in two different configurations. The first configuration referred to as HSRR1 consists of a square ring inside the circular ring while the second configuration referred to as HSRR2 consists of a circular ring embedded inside a square ring as shown in Figure 3 (a) and (d) respectively. The dimensions of these configurations are optimized to operate at 2.65 GHz and 4 GHz.

Simulated unit cells with proper boundary conditions and with their metamaterial characteristics are depicted in Figure 3 (a)-(c) and Figure 3 (d)-(f) respectively. For unit cell simulation, there are electric boundaries on the top and the bottom of each cell. To maintain electric boundaries for unit cell simulation, a metal strip is kept on the backside of the substrate. Magnetic boundaries are set at the front and the back of each cell because the magnetic field induced in the SRR is normal to the plane¹⁷.

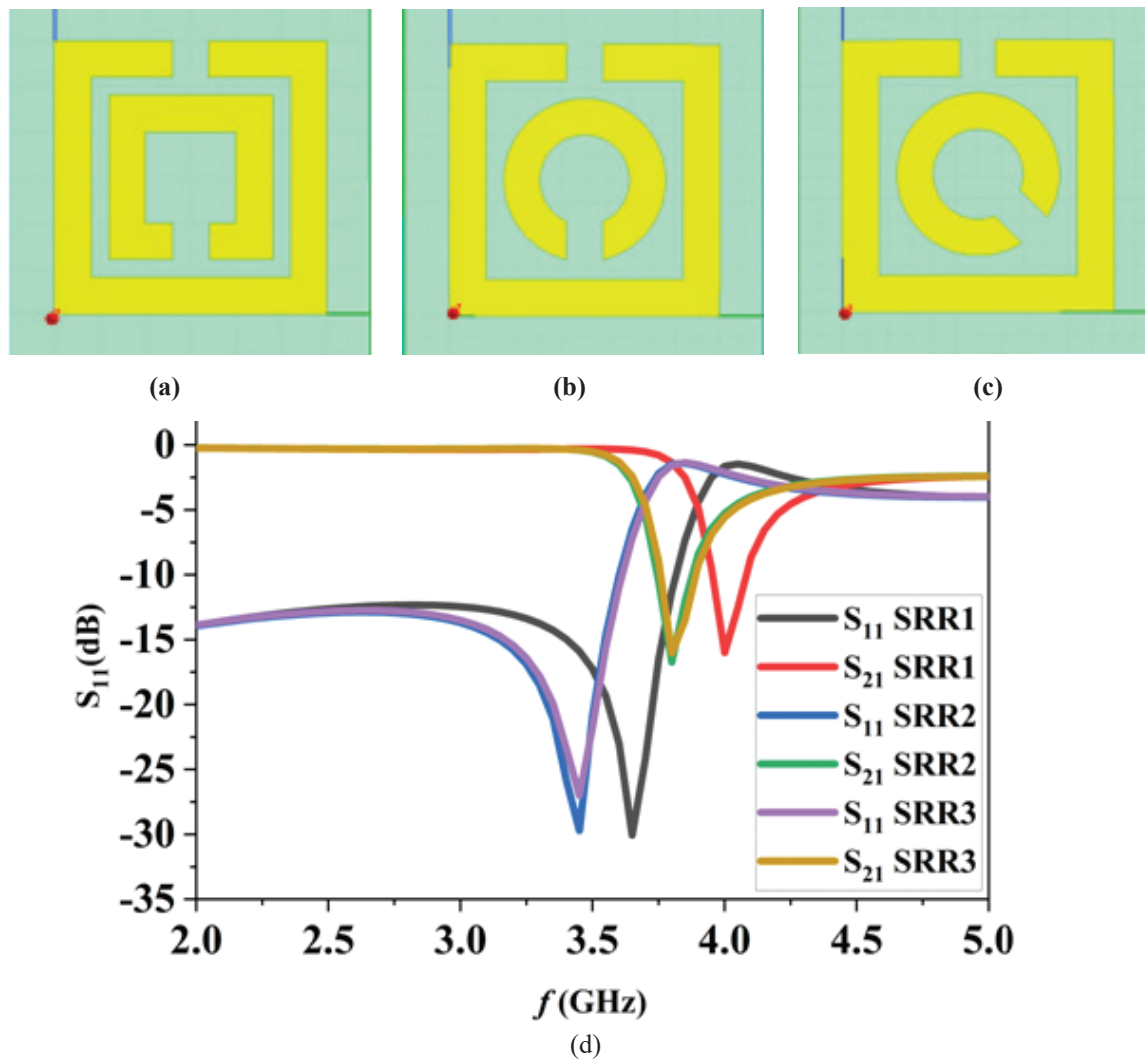


Figure 2. Evolution of hybrid SRR: (a) SRR 1, (b) SRR 2, (c) SRR 3, and (d) S11 and S21 coefficients for the unit cells.

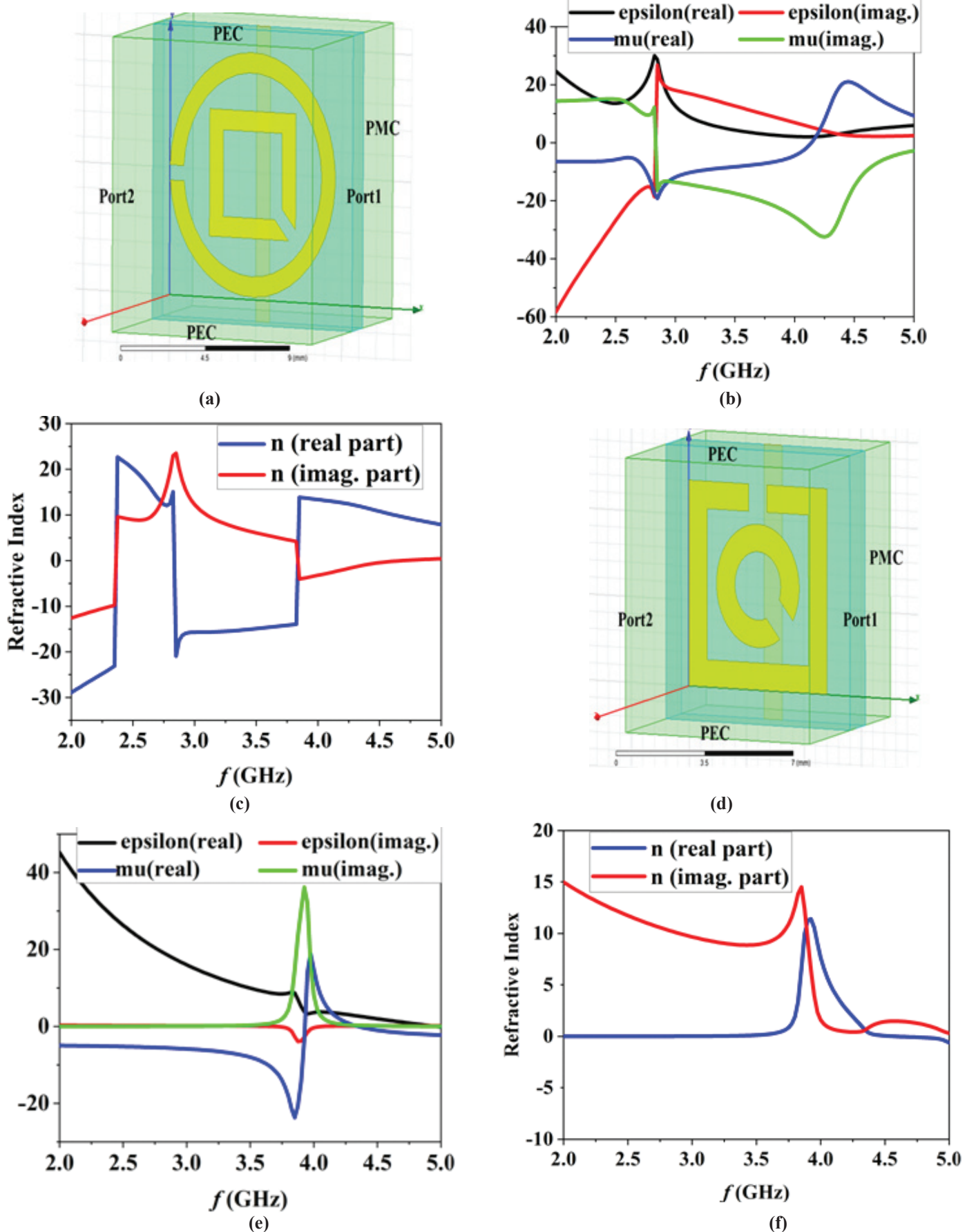


Figure 3. (a) Unit cell HSRR1, (b) Epsilon and mu values for HSRR1, (c) Refractive index for HSRR1, (d) Unit cell HSRR2, (e) Epsilon and mu values for HSRR2, and (f) Refractive index for HSRR2.

Then from the unit cell simulation, S_{11} and S_{12} parameters were extracted and used to calculate metamaterial characteristics for each unit cell in MATLAB³⁴. The calculated relative permittivity, permeability, and refractive index for these unit cells are displayed in Fig. 3. The negative refractive index verifies the metamaterial properties.

The resonant frequency of a unit cell is where the real part of its refractive index goes negative. From Fig.3 (b)-(c), it is visible that the real part of the permeability and the refractive index for HSRR1 is negative around 2.65 GHz which was expected. The refractive index for the second unit cell HSRR2 is shown in Fig. 3(f). After having a close observation of Fig. 3 (e)-(f), it is seen that the refractive index for HSRR2 is slightly negative in the region after 4.5 GHz, which is of our interest.

2.4 Design Strategy and Role of Hybrid-SRR

The unit cells designed above are used to convert a monopole antenna into a miniaturized triple-band antenna. The rectangular metallic strip on the top of the substrate acts as a monopole antenna, giving a single frequency band around 3.6 GHz in simulation results as shown in Fig. 4 (a) and Fig. 5. Now HSRR2 is introduced into the truncated ground plane, which provides an additional frequency band around 4.7 GHz, higher than the monopole antenna frequency. Again, HSRR1 is loaded on the truncated ground plane. This provides the third frequency band around 2.65 GHz, which is lower than the monopole antenna frequency band. These gradual developments are shown in Fig. 4 and Fig. 5 respectively.

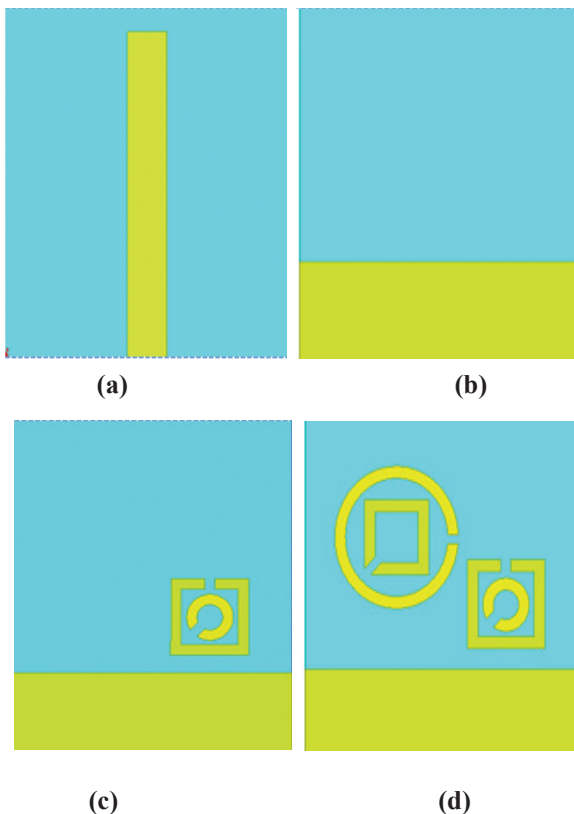


Figure 4. Antenna development by gradual modifications in ground plane: (a) Monopole antenna, (b) Ground plane stage 1, (c) Ground plane stage 2, and (d) Ground plane stage 3.

Finally, three frequency bands are achieved with the final design i.e. 2.6-2.7 GHz, 3.35-4.1 GHz, and 4.6-4.9 GHz. It is seen that loading of the HSRR1 at the ground plane giving additional lower band needs no alteration in the overall dimension of antenna, this is the beauty of the proposed design and benefit of using metamaterial inspired unit cells. In this way, multi-banding is performed and since this third band is in the lower frequency range than that of starting patch, miniaturization is done indirectly.

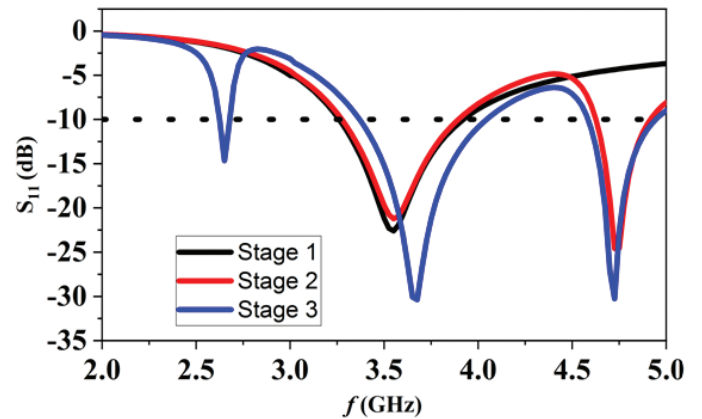


Figure 5. Comparison of reflection coefficient for the antenna at every stage.

Simulated plots for surface current distributions at various frequencies are also in the accordance with the antenna development (Fig. 6). It can be seen from Fig. 6(a) that HSRR1 is the active element at 2.65 GHz for which it was designed. The middle band is due to monopole antenna which is indicated in Fig. 6(b)-(c) at frequencies 3.65 GHz and 4GHz respectively. At 4.8 GHz, HSRR2 is the active element for which it was introduced.

3. RESULTS AND DISCUSSION

The image of the actual fabricated prototype antenna is displayed in Figure 7. Although FR4 is a lossy material because of its high relative permittivity value; one of the reasons for selecting substrate material as FR4 is due to its easy availability and low cost. These two parameters have a great impact on practical design implementation and manufacturing.

3.1 Reflection Coefficient (S-parameter)

The reflection coefficient (S_{11}) for the proposed antenna has been measured using Agilent's Vector Network Analyzer. A comparison of the simulated and the measured reflection coefficient is given in Fig. 8. The three frequency bands (for which $S_{11} < -10$ dB) achieved from the simulations are 2.6-2.7 GHz, 3.35-4.1 GHz, and 4.6-4.9 GHz, and the corresponding frequency bands yielded from the measured values are 2.72-2.83 GHz, 3.54-4.35 GHz, and 4.72-5 GHz respectively. Hence, the proposed antenna shows a significant amount of impedance bandwidth of 4%, 20%, and 6% for the respective three frequency bands 2.8/4/4.8 GHz, which makes the proposed design a good candidate for wireless applications. The measured results closely approximate the simulated ones, with a very small difference of about 5.6%. Fabrication inaccuracies such as mask scaling and misalignment may be the possible reasons for the slight mismatch in the results.

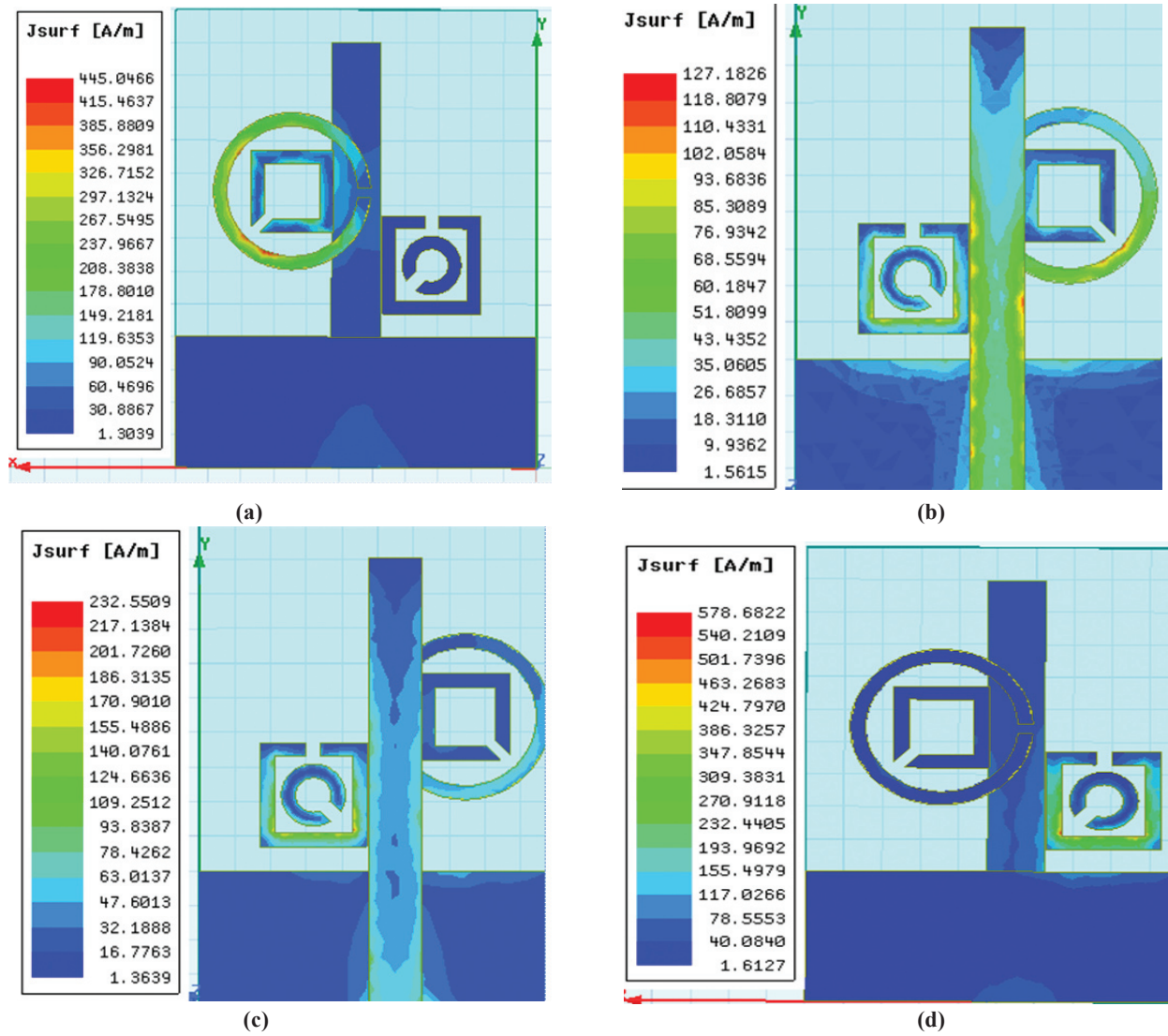


Figure 6. Simulated surface current distribution at: (a) 2.65 GHz, (b) 3.65 GHz, (c) 4 GHz, and (d) 4.8 GHz.

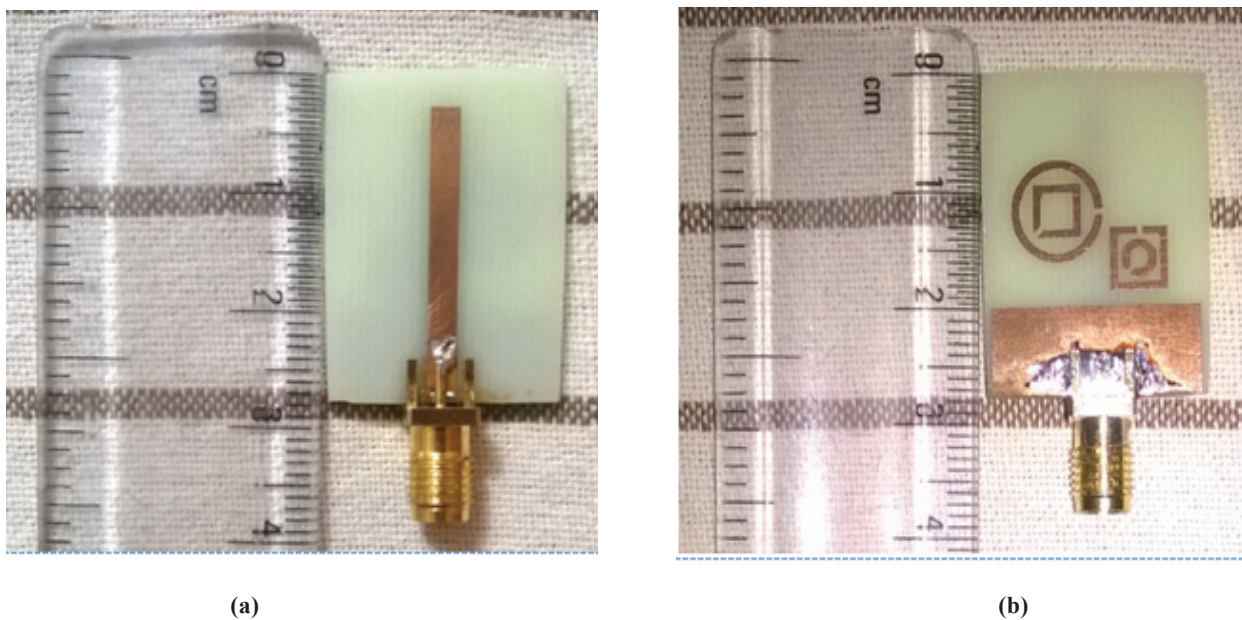


Figure 7. Fabricated prototype of antenna: (a) Top view, and (b) Bottom view.

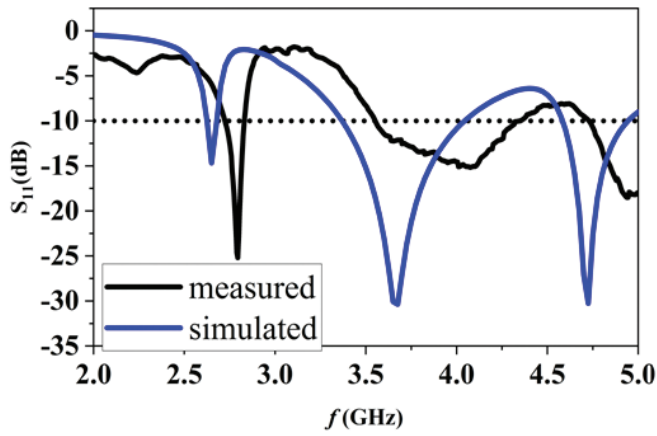


Figure 8. Comparison of simulated and measured reflection coefficient (S_{11}) for the proposed antenna.

3.2 Gain

The measurement of gain of the antenna is carried out in an anechoic chamber. Horn antenna is used as a reference antenna in the measurement and the test antenna is placed at a

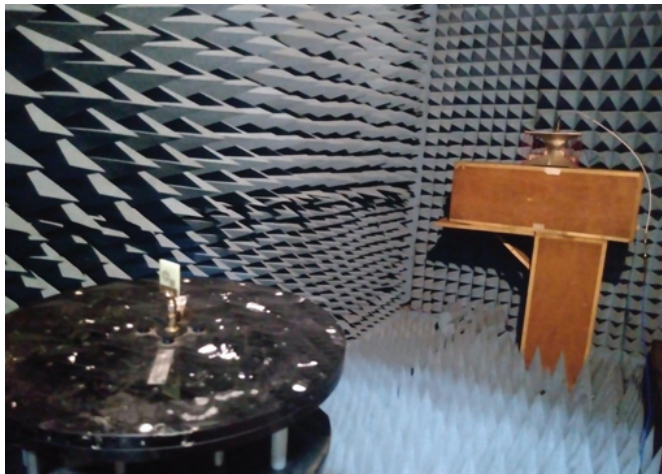


Figure 9. Setup for gain measurement.

distance of 2.25 meters from the reference antenna. The setup for gain measurement is shown in Fig. 9.

Gain is the measurement of radiation characteristics and functionality of the antenna. The normalized values of the measured and the simulated gain patterns for the prototype antenna are plotted in Figure 10 with the peak simulated gain values of -0.9310 dBi, 2.6739 dBi, and 2.6596 dBi at 2.8 GHz, 4 GHz, and 4.8 GHz respectively. The radiation pattern is almost omnidirectional in the XZ plane.

An extensive literature survey has been done for this research work for its proper placing among contemporary techniques. A comparative analysis is given in Table 2, showing the relevance of the proposed work.

It is observed from Table 2, that the proposed antenna is a better choice in terms of multiple bands, bandwidth, and compact size. Also, despite the narrow-band characteristics of metamaterial unit cells, this antenna yields a larger bandwidth in comparison to other antenna mentioned in Table 2. The proposed antenna uses FR4 substrate which is not expensive.

4. CONCLUSION

A triple-band antenna for different S-band and C-band applications is designed, fabricated, and characterized. The novelty of the proposed design lies in the use of hybrid-SRRs and the indirect miniaturization caused by HSRR1. The footprint of the developed antenna is reduced by 60 %. The prototype antenna functionally radiates at three frequency bands viz. 2.8/4/4.8 GHz, having a bandwidth of 4 %, 20 %, and 6 % respectively. Hence, the proposed design serves both of its purposes miniaturization as well as multi-banding. The proposed antenna has a robust design due to the use of metamaterial-inspired hybrid-SRRs which reduces complexity and gives ease of optimization control, as illustrated in section two. This design is engraved upon an inexpensive FR4 substrate. A detailed and step-by-step analysis is done for design methodology and metamaterial concepts which could be useful for other future applications too.

Table 2 Comparative study

Ref.	Size ($\lambda_0 \times \lambda_0$)	Frequency bands (GHz)	Bandwidth (GHz)	Substrate	Metamaterial property	Year
[2]	0.20×0.20	1.5/3.5/5.4	0.8	FR4	Not verified	2017
[10]	0.26×0.27	2.6/3.5/4.85	0.90	FR4 +Air	NA	2021
[22]	0.22×0.27	1.65/1.93/2.20	0.41	FR4	Not verified	2014
[24]	0.29×0.29	1.72/2.17	0.65	FR4	Not verified	2015
[25]	0.25×0.25	2.5/3.5/5.2	NA	FR4	Not verified	2015
[26]	0.20×0.36	1.54/1.63/2.25/3.69	0.5	Rogers Duroid	Not verified	2016
[27]	0.23×0.35	3.5/5.8	0.8	Fr4	Not verified	2017
[29]	0.20×0.20	3.2, 5.4, 5.8	0.26	Neltec	verified	2018
[30]	0.43×0.46	5/6.8	0.6	Fr4	Not verified	2019
[31]	0.29×0.29	2.4	0.08	Fr4 and F4B-2	Not verified	2020
[32]	0.19×0.21	3.2/4/5.9	0.35	RT Duroid	verified	2021
Proposed Antenna	0.19×0.25	2.8/4.0/4.8	1.20	Fr4	verified	2021

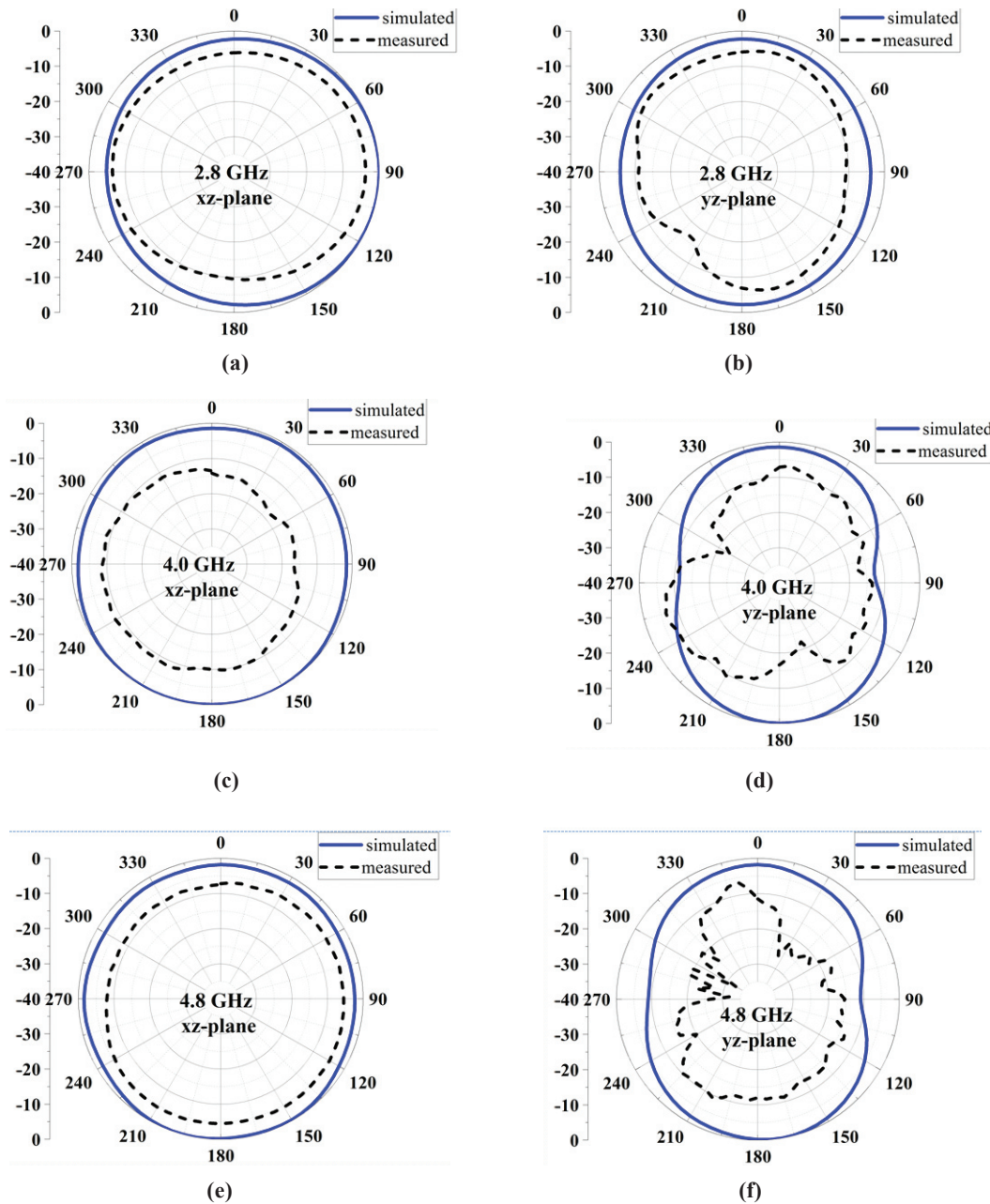


Figure 10. Simulated and measured gain over all three bands: (a)-(b) at 2.8 GHz, (c)-(d) at 4 GHz, and (e)-(f) at 4.8 GHz.

ACKNOWLEDGMENTS

This research work is supported by the Ministry of Electronics & Information Technology (MeitY), Government of India, under the Visvesvaraya PhD Scheme.

REFERENCES

1. Fallahpour, M.; Zoughi, R. Antenna Miniaturization Techniques: A Review of Topology and Material Based Method. *IEEE Antennas Propag. Mag.*, 2018, **60**(1), 38-50. doi: 10.1109/MAP.2017.2774138
2. Rajabloo, H.; Kooshki, V.A. & Oraizi, H. Compact microstrip fractal Koch slot antenna with ELC coupling load for triple band application. *Int. J. Electron Commun. (AEU)*, 2017, **73**, 144-149. doi: 10.1016/J.AEUE.2016.12.027
3. Beigi, P. & Mohammadi, P. A novel small triple-band monopole antenna with crinkle fractal-structure. *Int. J. Electron Commun.(AEU)*, 2016, **70**(10), 1382-1387. doi: 10.1016/J.AEUE.2016.07.013
4. Yazdani, R.; Yousefi, M.; Aliakbarian, H.; Oraizi, H. & Vandenbosch, G.A.E. Miniaturized Triple-Band Highly Transparent Antenna. *IEEE Trans. Antennas Propag.*, 2020, **68**(2), 712-718. doi: 10.1109/TAP.2019.2947132
5. Iwamoto, K.; Kimura, Y.; Saito, S. & Kimura, Y. Design of a Triple-band and Wideband Multi-Ring Microstrip Antenna fed by an L-probe. In Proceedings of the ISAP 2020, Osaka, Japan, 2020. doi: 10.23919/ISAP47053.2021.9391166
6. Sun, Xiaolei L.; Cheung, S. W. & Yuk, T. I. Design of Compact Antenna for 2.4/4.9/5.2/5.8- GHz WLAN.

- Microw. Opt. Technol. Lett.*, 2014, **56**(6), 1360-1366.
doi: 10.1002/MOP.28368
7. Trong, Tuan-Anh Le *et al.* A Compact triple-band antenna with a broadside radiation characteristic for head-implantable wireless communication. *IEEE Antennas Wireless Propag. Lett.*, 2021, **20**(6), 958-962.
doi: 10.1109/LAWP.2021.3068170
 8. Al-Mihrab, Mohammed A. *et al.* A compact multiband printed monopole antenna with hybrid polarization radiation for GPS, LTE and satellite applications. *IEEE Access*, 2020, **8**, 110371-110380.
doi: 10.1109/ACCESS.2020.3000436
 9. Peng, Mei *et al.* Design of a triple-band shared-aperture antenna with high figures of merit. *IEEE Trans. Antennas Propag.*, 2021, **69**(12), 8884-8889.
doi: 10.1109/TAP.2021.3090837
 10. Chang, Le; Zhang, G. & Wang, H. Triple -Band microstrip microstrip patch antenna and its Four -Antenna Module Based on Half -Mode Patch patch for 5G 4×4 MIMO Operation. *IEEE Trans. Antennas Propag*, 2021, **70**(1), 67-74.
doi: 10.1109/TAP.2021.3090572
 11. Veselago, V.G. The electrodynamics of substances with simultaneously negative values of epsilon and mu. *Sov. Phys. Uspekhi*, 1968, **10**, 509-514.
doi: 10.1070/PU1968V010N04ABEH003699
 12. Pendry, J.B.; Holden, A.J.; Robbins, D.J. & Stewart, W.J. Low frequency plasmons in thin wire structures. *J. Phys.: Condens. Matter*, 1998, **10**, 4785-4788.
doi: 10.1088/0953-8984/10/22/007
 13. Pendry, J.B.; Holden, A.J.; Robbins, D.J. & Stewart, W.J. Magnetism from conductors and enhanced nonlinear phenomena. *IEEE Trans. Microw. Theory Tech.*, 1999, **47**, 2075-2081.
doi: 10.1109/22.798002
 14. Shelby, R.A.; Smith, D.R. & Schultz, S. Experimental verification of a negative Index of refraction. *Science Magazine*, 2001, **292**(5514), 77-79.
doi: 10.1126/SCIENCE.1058847
 15. Smith, D.R.; Schultz, S.; Markos, P. & Soukoulis, C.M. Determination of effective permittivity and permeability of metamaterials from reflection and transmission coefficients. *Physical Review B*, 2002, **65**(19).
doi: 10.1103/PhysRevB.65.195104
 16. Hrbar, S. & Bartolic, J. Simplified analysis of split ring resonator used in Backward meta-material. *In Proceedings of the MMEP 02*, 2002.
doi: 10.1109/MMET.2002.1107013
 17. Ziolkowski, R.W. Design, fabrication, and testing of double negative metamaterials. *IEEE Trans. Antennas Propag*, 2003, **51**(7), 1516-1529.
doi: 10.1109/TAP.2003.813622
 18. Ramakrishna, S.A. Physics of negative refractive index materials. *Rep. Prog. Physics*, 2005, **68**, 449-521.
doi: 10.1088/0034-4885/68/2/R06
 19. Engheta, N. & Ziolkowski, R.W. *Metamaterials: Physics and engineering exploration*. IEEE Press, 2006. ISBN: 978-0-471-76102-0
 20. Cheribi, H.; Ghanem, F. & Kimouche, H. Metamaterial-Based Frequency Reconfigurable Antenna. *Electronics Letters*, 2013, **49**(5), 315-346.
doi: 10.1049/EL.2012.3651
 21. Huang, He; Liu, Ying; Zhang, Shaoshuai & Gong Shuxi. Multiband Metamaterial-Loaded Monopole Antenna for WLAN/WiMAX Applications. *IEEE Antennas Wireless Propag. Lett.*, 2015, **14**, 662-665.
doi:10.1109/LAWP.2014.2376969
 22. Sarkar, D.; Saurav, K. & Srivastava, K.V. Multi-band microstrip-fed slot antenna loaded with split-ring resonator. *Electron. Lett.*, 2014, **50**(21), 1498-1500.
doi: 10.1049/EL.2014.2625
 23. Patel, S.K. & Kosta, Y. Complementary split ring resonator metamaterial to achieve multifrequency operation in microstrip-based radiating structure design. *J. Mod. Opt.*, 2014, **61**(3), 249-256.
doi: 10.1080/09500340.2013.879938
 24. Sharma, S.K. & Chaudhary, R.K. Dual-band metamaterial-inspired antenna for mobile applications. *Microw. Opt. Technol. Lett.*, 2015, **57**(6), 1444-1447.
doi: 10.1002/MOP.29113
 25. Shehata, G.; Mohanna, M. & Rabeh, M.L. Triband small monopole antenna based on SRR units. *NRIAG J. Astron. Geophys.*, 2015, **4**(2), 185-191.
doi: 10.1016/j.nrjag.2015.08.003
 26. Dakhli, S.; Rmili, H.; Floc'h, J.M.; Sheikh, M.; Dobaie, A.; Mahdjoubi, K.; Choubani, F. & Ziolkowski, R.W. Printed multiband metamaterial inspired antennas. *Microw. Opt. Technol. Lett.*, 2016, **58**(6), 1281-1289.
doi: 10.1002/mop.29792
 27. Yu, Kai; Li, Y. & Wang, Y. Multi-band metamaterial-based microstrip antenna for WLAN and WiMAX applications. *In Proceedings of the Symposium ACES 2017*, Italy, 2017.
doi: 10.23919/ROPACES.2017.7916032
 28. Sarkar, D. & Srivastava, K.V. Compact four-element SRR loaded dual band MIMO antenna for WLAN/WiMAX/WiFi/4G-LTE and 5G applications. *Electron. Lett.*, 2017, **53**, 1623-1624.
doi: 10.1049/EL.2017.2825
 29. Singh, A.K.; Abegaonkar, M.P. & Koul, S.K. Miniaturized multiband microstrip patch antenna using metamaterial loading for wireless applications. *Prog. Electromagn. Res. C*, 2018, **83**, 71-82.
doi: 10.2528/PIERC18012905
 30. Bora, P. & Paul, C. Metamaterial loaded CSRR based antenna for WLAN and IOT BAND applications. *Int. J. Sci. Technol. Res.* 2019, **8**(9), 2060-2065. <https://www.ijstr.org/final-print/sep2019/Metamaterial-Loaded-Csrr-Based-Antenna-For-Wlan-And-Iot-Band-Applications-.pdf> [Accessed on 23 June 2022]
 31. Wang, Zhan *et al.* Compact omnidirectional antenna using SRR for WiFi application. *In Proceedings of the IEEE International Symposium on Antennas and Propagation and North American Radio Science Meeting 2020*, Montreal, QC, Canada, 2020
doi: 10.1109/IEEECONF35879.2020.9329943

32. David, Rajiv Mohan; Saadh, AW Mohammad; Ali, T. & Kumar, Pradeep. A multiband antenna stacked with novel metamaterial SCSRR and CSSRR for WiMAX/WLAN applications. *Micromachines*, 2021, **12**(2), 113. doi: 10.3390/mi12020113
33. Setia, V.; Sharma, K.K. & Koul, S.K. Triple-Band metamaterial inspired microstrip antenna using split ring resonators for WLAN/WiMAX applications. *In Proceedings of the IEEE Indian Conference on Antennas and Propagation 2019, Ahmedabad, India, 2019.* doi: 10.1109/InCAP47789.2019.9134602
34. Numan, A.B. & Sharawi, M.S. Extraction of material parameters for metamaterials using a full-wave simulator. *IEEE Antennas Propag. Mag.*, 2013, **55**(5), 202-211. doi: 10.1109/MAP.2013.6735515

CONTRIBUTORS

Mr Varun Setia received B.Tech degree in Electronics and Communication Engineering from College of Technology, G.B. Pant University of Agriculture & Technology, Pantnagar (Uttarakhand), India, in 2006, and M.Tech degree from the National Institute of Technology, Hamirpur (H.P.), India, in 2011. He is currently pursuing a PhD at MNIT Jaipur, India. His research interests include metamaterial surfaces & unit cells, microstrip antenna, microwave devices, and image compression. In the present work, he developed the design and prepared the initial draft of the manuscript.

Dr Kamalesh Kumar Sharma received the BE and ME degrees in Electronics and Communication Engineering from Malaviya National Institute of Technology, Jaipur, India, in 1990 and 2001, respectively. He completed his PhD degree from IIT Delhi in the year 2008. Presently, he is working as Professor (HAG) with the Department of Electronics and Communication Engineering, Malaviya National Institute of Technology. His research interests include electromagnetics, antenna design, sampling theory of signals, signal and image processing and fractional Fourier transforms. In the present work, he guided the simulation work and revised the manuscript.

Dr Shibhan Kishan Koul received the BE degree in electrical engineering from Regional Engineering College, Srinagar, India, in 1977, and the M.Tech and PhD degrees in microwave engineering from the Indian Institute of Technology Delhi, New Delhi, India, in 1979 and 1983, respectively. He has been an Emeritus Professor with the Indian Institute of Technology Delhi, since 2019, and the Mentor Deputy Director (Strategy & Planning, International affairs) of IIT Jammu, Jammu and Kashmir, India, since 2018. His research interests include RF MEMS, optical and millimetre wave dielectric integrated guides and circuits, medical applications of sub-terahertz waves, reconfigurable microwave circuits, and miniaturized antennas. He holds 26 patents, six copyrights, and one trademark. In the present work, he provided the conceptual framework, and supervised the experimental findings.